Earthline Journal of Chemical Sciences
E-ISSN: 2581-9003; CODEN: EJCSB4
Volume 13, Number 1, February 2026, Pages 43-63
https://doi.org/10.34198/ejcs.13126.04.043063

Some isomers of BN-embedded phenanthrene – A DFT treatment

Lemi Türker

Department of Chemistry, Middle East Technical University, Üniversiteler, Eskişehir Yolu No: 1, 06800 Çankaya/Ankara, Turkey
e-mail: lturker@gmail.com; lturker@metu.edu.tr

Abstract

Boron–nitrogen heteroarenes possess great promise for practical application in many areas of chemistry, biochemistry and pharmacology, beside materials science, and transition-metal-based catalysis. Presently, various BN-bond having phenanthrenes have been investigated thoroughly within the constraints of density functional theory at the level of B3LYP/6-311++G(d,p). The collected data have revealed that the optimized structures of them have exothermic heats of formation and favorable Gibbs free energy of formation values. They are thermally favored and electronically stable at the standard states. Various structural and quantum chemical data have been collected and discussed, including IR and UV-VIS spectra. Also "nucleus-independent chemical shift" (NICS) data have been presented for each ring.

1. Introduction

The past years have witnessed emergence of some advances of organic conjugated materials and then great enthusiasm pushed scientists to develop some novel π-molecules. They searched application of them to organic electronic devices, e.g., organic field effect transistors (OFETs) [1,2], organic light emitting diodes (OLEDs) [3], organic solar cells (OSCs) [4, 5], organic thermoelectric devices (OTEDs) [6-8], and organic photo detectors (OTDs) [9-11].

Among aromatic compounds, borazaenes represent a significant class of isosteres in which carbon - carbon bonds have been replaced by B−N bonds. Boron–nitrogen heteroarenes hold great promise for practical application in many areas of chemistry, such as BN-heterocycles in biochemistry and pharmacology, materials science, and transition-metal-based catalysis [12].

The replacement of two carbon atoms in a benzene ring with one boron and one nitrogen atom can proceed according to three permutations to produce 1,2-dihydro-1,2-azaborine, 1,3-dihydro-1,3-azaborine, or 1,4-dihydro-1,4-azaborine.

The total electronic number of two carbons (12e) is equal to the electronic sum of one boron (5e) and one nitrogen (7e). Accordingly, replacing two carbons with one boron and one nitrogen in a π-conjugated structure gives an isoelectronic system, i.e., the BN perturbed π-conjugated system, comparing to their all-carbon analogs.

The BN-embedded π-conjugated systems have unique properties, e.g., optical absorption, emission, energy levels, band gaps, and packing order in contrast to their all-carbon analogs and have been intensively studied in terms of novel synthesis, photo physical characterizations, and electronic applications in recent years [13].

The first wave of BN-heteroarene research began in the late 1950s with Dewar's studies of polycyclic

Received: November 16, 2025; Accepted: December 12, 2025; Published: December 16, 2025

Keywords and phrases: BN-embedded phenanthrene, isoelectronic structure, spectra, NICS, DFT calculations.

derivatives of BN-naphthalenes, phenanthrene, and tetraphenes. The early syntheses of these compounds often employed harsh conditions and afforded products in low overall yields [12]. The photoisomerization [14] and Diels-Alder cycloaddition [15] of 1,2-azaborines to form heteroatom-substituted cyclobutane and cyclohexane derivatives, respectively, represent promising initial leads toward this development.

The azaborine unit is also being investigated in medicinal chemistry as a new pharmacophore with unique pharmacokinetic profiles. Azaborine-containing ligands have also recently been shown to support distinct modes of reactivity and selectivity in transition-metal-based catalysis [1].

For B-N covalent bond embedded π-conjugated units, they are suitable to act as electron-rich units to construct electron-donor materials owing to their high-lying energy levels, good backbone co-planarity, and high hole mobility. However, their absorption bands should be further broadened to lower energy (600–800 nm) to enhance the light harvesting ability [13].

Up to date, 1,2-azaborine and its π-extended conjugated molecules have been widely studied and thoroughly reviewed [16-22]. In the present density functional (DFT) study, some isomers of BN-bond embedded phenanthrene are considered at the molecular level.

2. Method of Calculations

In the present study, all the initial optimizations of the structures leading to energy minima have been achieved first by using MM2 method which is then followed by semi empirical PM3 self consistent fields molecular orbital method [23-25]. Afterwards, the structure optimizations have been achieved within the framework of Hartree-Fock and finally by using density functional theory (DFT) at the level of B3LYP/6-311++G(d,p) [26,27]. Note that the exchange term of B3LYP consists of hybrid Hartree-Fock and local spin density (LSD) exchange functions with Becke's gradient correlation to LSD exchange [28]. The correlation term of B3LYP consists of the Vosko, Wilk, Nusair (VWN3) local correlation functional [29] and Lee, Yang, Parr (LYP) correlation correction functional [30]. In the present study, the normal mode analysis for each structure yielded no imaginary frequencies for the $3N–6$ vibrational degrees of freedom, where N is the number of atoms in the system. This search has indicated that the structure of each molecule considered corresponds to at least a local minimum on the potential energy surface. Furthermore, all the bond lengths have been thoroughly searched in order to find out whether any bond cleavages occurred or not during the geometry optimization process. All these computations were performed by using SPARTAN 06 program [31]. Whereas the nucleus-independent chemical shift, NICS(0), calculations have been performed by using Gaussian 03 program [32].

3. Results and Discussion

Phenanthrene is an even alternant hydrocarbon [33,34] having equal numbers of starred and unstarred positions. Even-alternant hydrocarbon structures are characterized with symmetrical location of occupied and unoccupied molecular orbital energy levels about zero energy level. However, centric perturbations involving carbon to heteroatom replacement lowers both of the occupied and unoccupied molecular orbital energy levels depending on the position of the perturbation (starred or unstarred position) and the character of the heteroatom [33,34].

Note that all the structures presently considered are in neutral form and in singlet state and they fall into two isomeric classes: $C_{12}H_8BN$ (structures 1,6,7,8,9) and $C_{12}H_{10}BN$ type isomers (structures 2,3,4,5,10,11),

respectively. In some cases, the boron atom is on the fusion point (2,4,10,11) and boron is on the peripheral circuit (1,3,5,6,7,8,9). Moreover, structures-3 and 5 contain B-H bond.

Figure 1 shows the optimized structures of the systems of consideration. The arrows stand for the direction of calculated dipole moment vectors. Note that a resultant dipole moment vector is the vectorial sum of the individual bond dipoles, thus location of the heteroatoms greatly affects both the magnitudes and the directions.

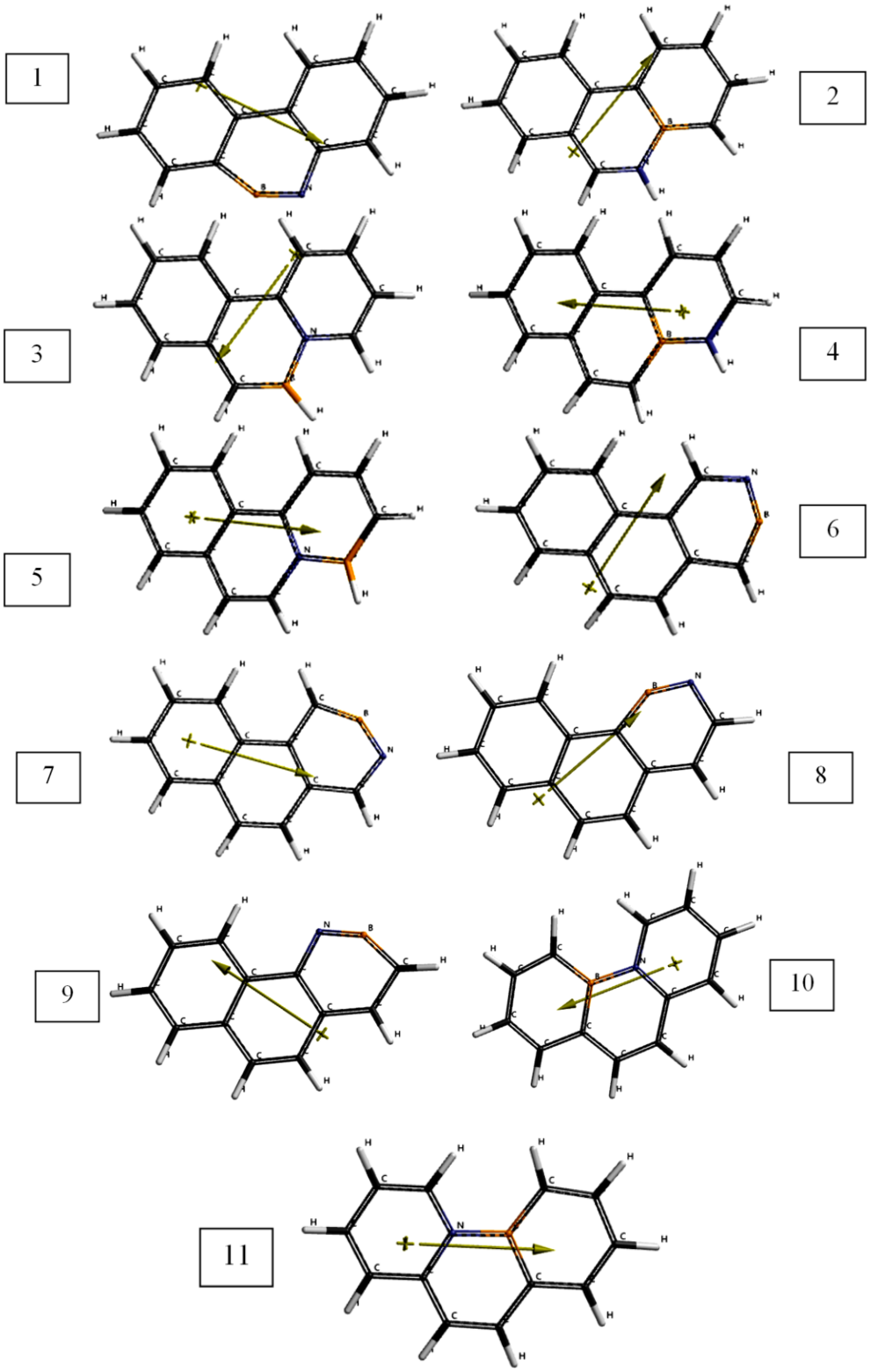

Figure 1. Optimized structures of the systems of consideration.

Figure 2 shows the calculated bond lengths of the structures considered. Some of the structures are highly interrelated through some symmetry operations, e.g., structures 10 and 11.

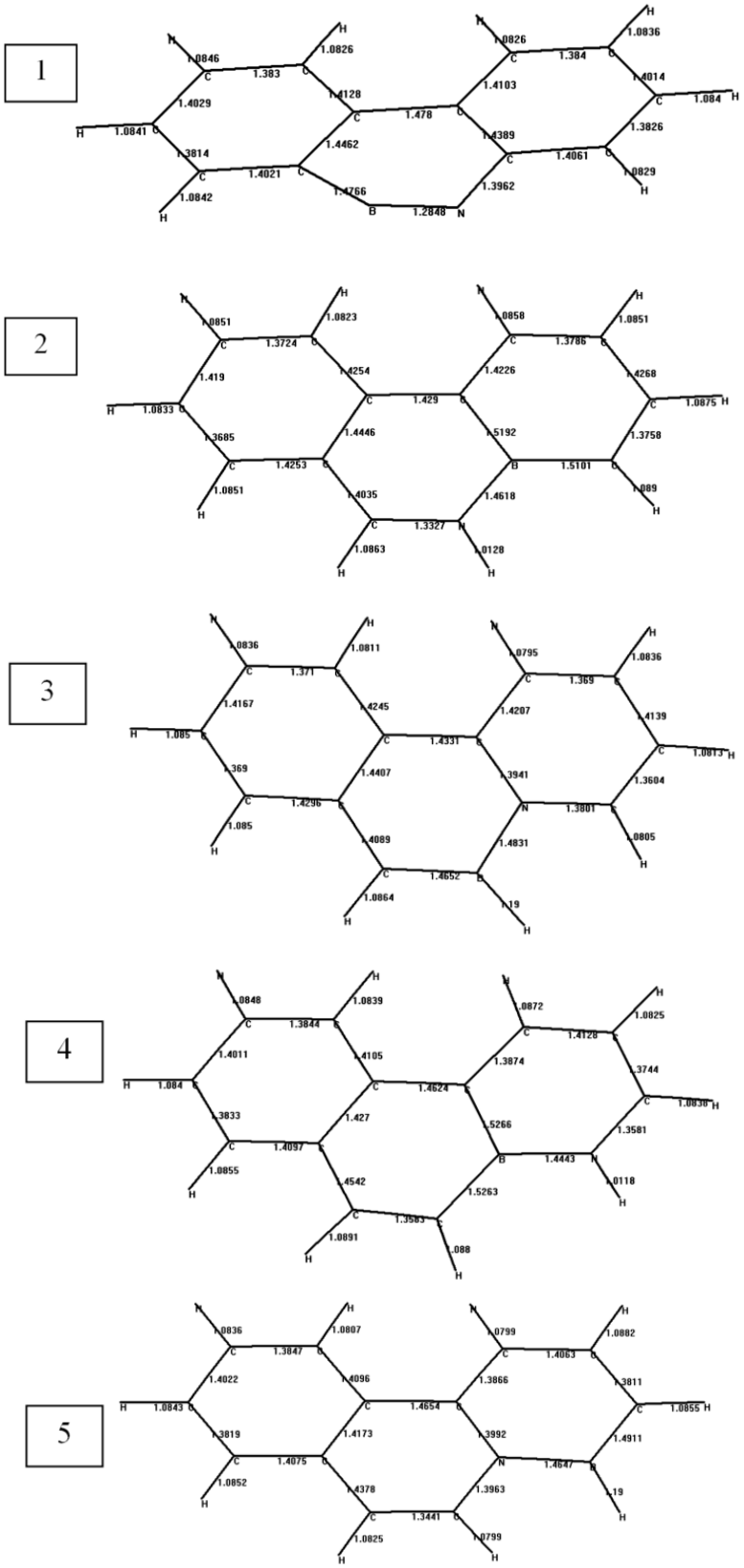

6

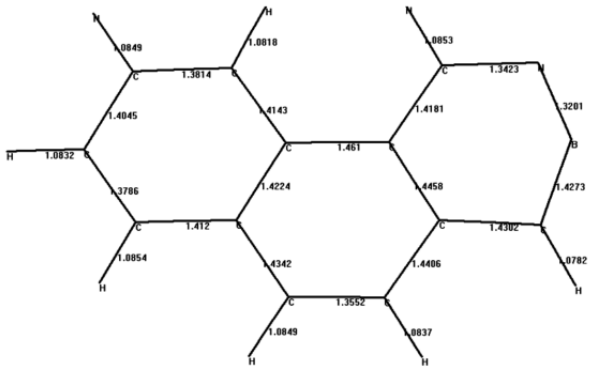

7

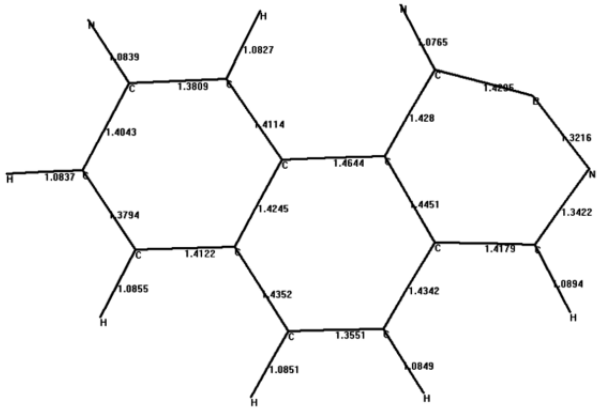

8

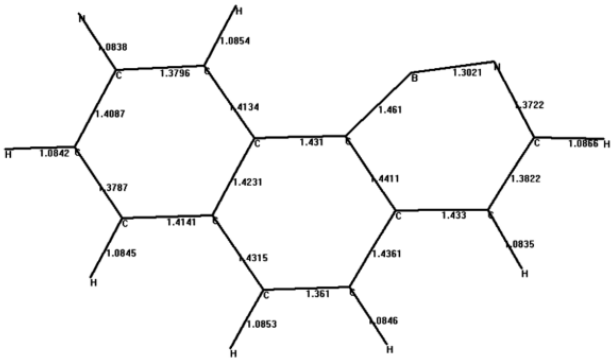

9

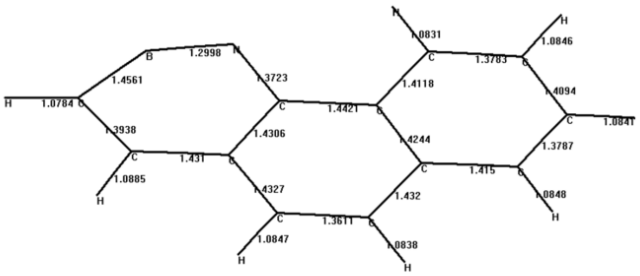

10

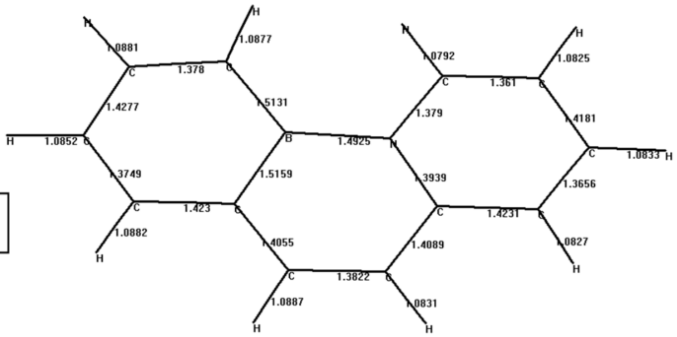

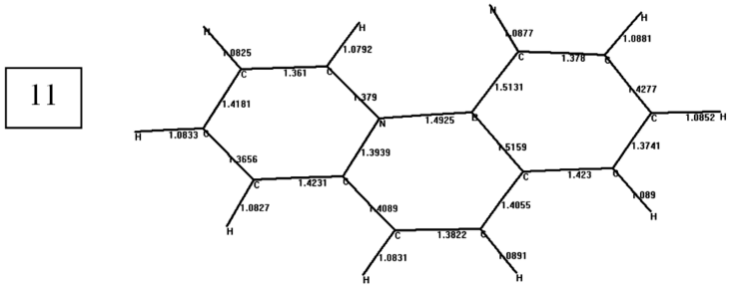

Figure 2. Calculated bond lengths of the structures considered.

Some thermo chemical properties of the structures considered are listed in Table 1. The data presented in the table reveal that the standard thermo chemical formation data of all the species considered are exothermic (H^o values) and they are favored according to their G^o (Gibbs free energy of formation) values. Structures 1,6,7,8,9 and 2,3,4,5,10,11 are $C_{12}H_8BN$ and $C_{12}H_{10}BN$ types, respectively. Note that in structures 2,4,10 and 11, the boron atom is on the fusion points. Note that $C_{12}H_{10}BN$ isomers, (2,3,4,5,10,11) are more exothermic and more stable than the isomers of $C_{12}H_8BN$ type (1,6,7,8,9). The algebraic orders of H^o and G^o values within the same type isomers is 9<1<8<7<6 for $C_{12}H_8BN$ types and 4<2<5<10=11<3 for $C_{12}H_{10}BN$ isomers.

Some energies of the structures considered are included in Table 2, where E, ZPE and E_C stand for the total electronic energy, zero point vibrational energy and the corrected total electronic energy, respectively. According to the data, all the structures are electronically stable. The algebraic order the stabilities are 9<1<8<7<6 for $C_{12}H_8BN$ types and 4<6<2<10=11<3 for $C_{12}H_{10}BN$ isomers.

Table 1. Some thermo chemical properties of the structures considered.

No	H^o	S^o (J/mol^o)	G^o
1	-1422114.482	138.71	-1422230.11
2	-1425370.357	392.28	-1425487.317
3	-1425324.592	390.14	-1425440.913
4	-1425403.497	392.18	-1425520.427
5	-1425357.077	390.10	-1425473.386
6	-1422088.374	387.69	-1422203.965
7	-1422092.343	386.97	-1422207.720
8	-1422111.113	388.57	-1422226.967
9	-1422119.210	387.21	-1422234.660
10	-1425341.351	391.85	-1425458.184
11	-1425341.351	391.85	-1425458.184

Energies in kJ/mol.

Table 2. Some energies of the structures considered.

No	E	ZPE	E_C
1	-1422568.11	440.75	-1422127.36
2	-1425887.31	503.56	-1425383.75
3	-1425836.95	499.20	-1425337.75
4	-1425921.39	504.48	-1425416.91
5	-1425870.12	499.91	-1425370.21
6	-1422541.00	439.66	-1422101.34
7	-1422544.82	439.59	-1422105.23
8	-1422563.93	440.08	-1422123.85
9	-1422571.53	439.52	-1422132.01
10	-1425856.45	501.81	-1425354.64
11	-1425856.45	501.81	-1425354.64

Energies in kJ/mol.

Figure 3 displays the ESP charges on the atoms of the structures considered. The ESP charges are obtained by the program based on a numerical method that generates charges that reproduce the electrostatic potential field from the entire wavefunction [31].

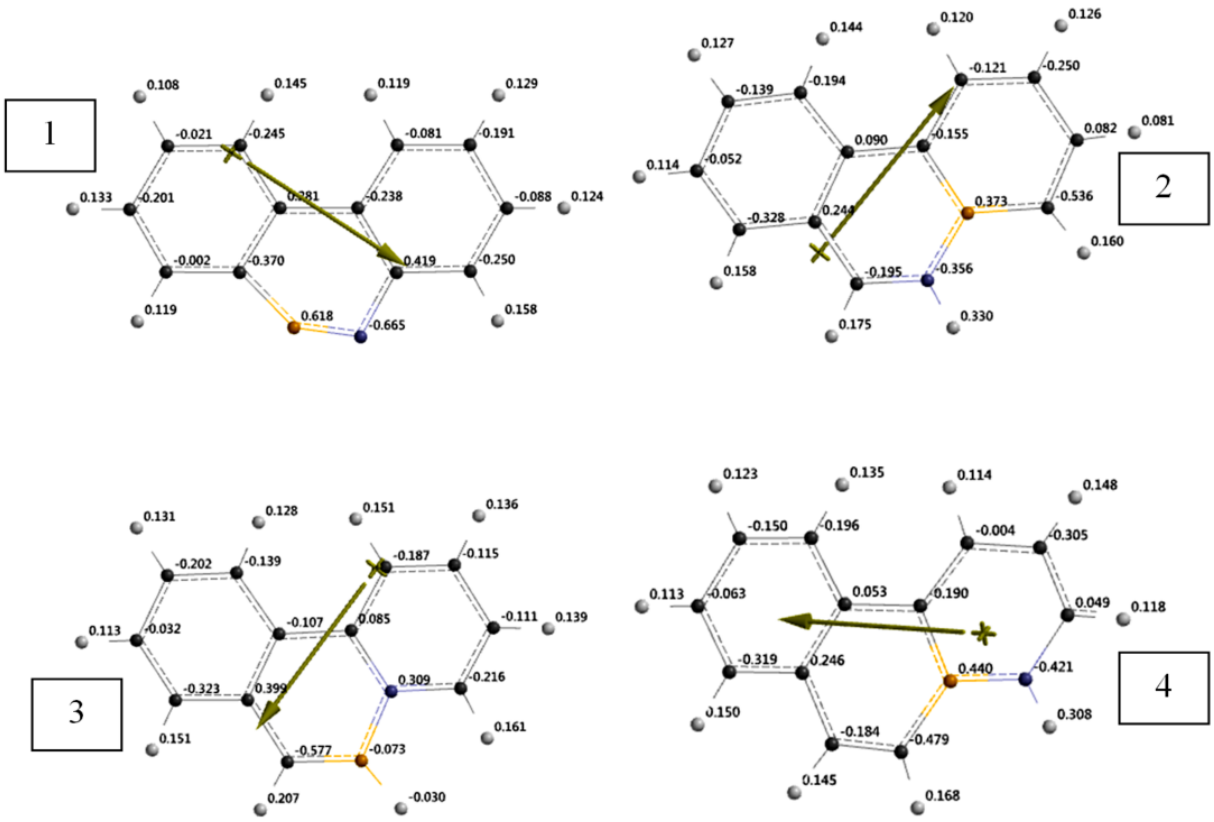

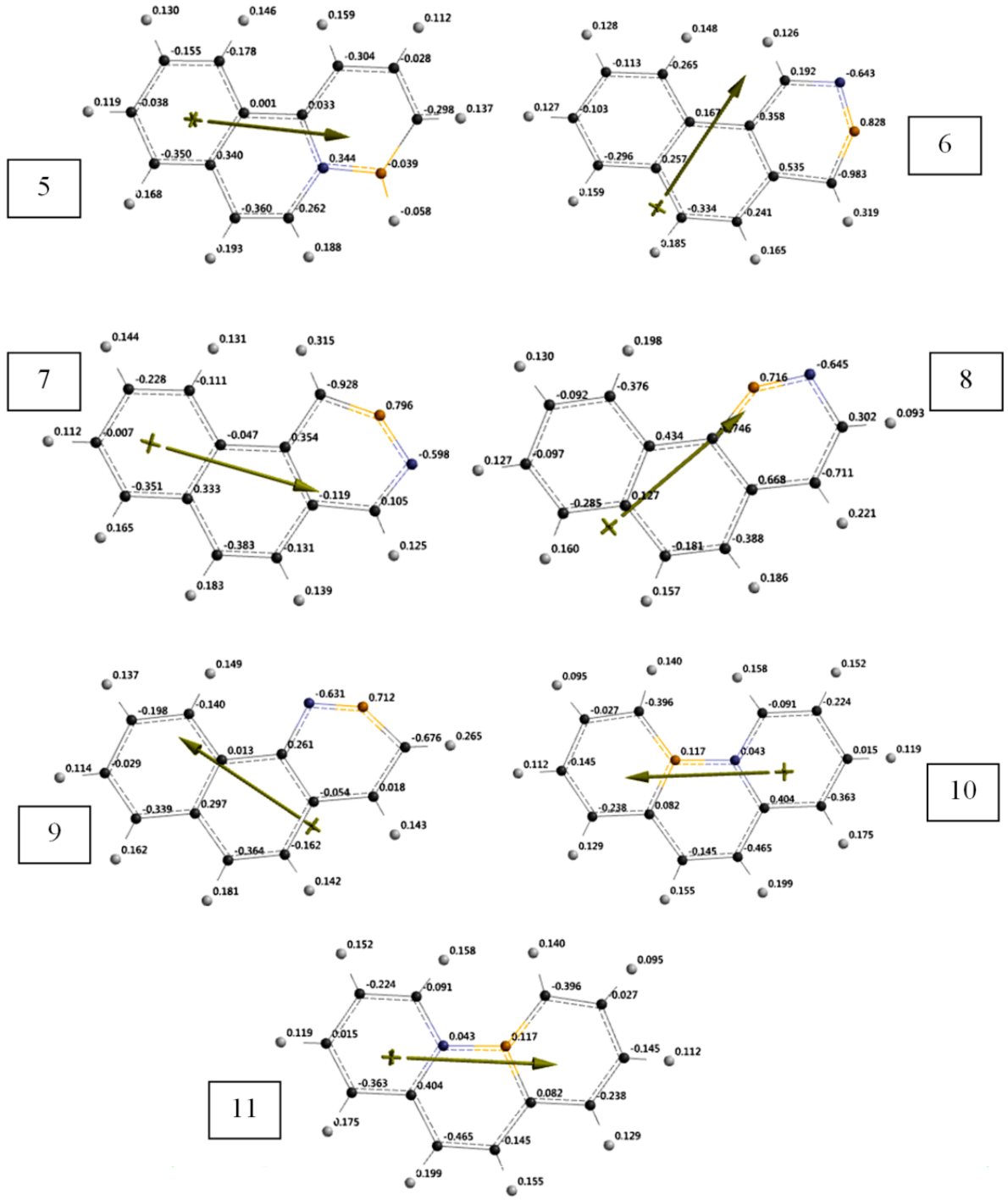

Figure 3. The ESP charges on the atoms of the structures considered.

Figure 3 reveals that ESP charge of the boron atom is positive except the ones in structures 3 and 5 (always positive at the fusion points) where the boron atom occupies the peripheral position ($C_{12}H_{10}BN$ isomers). Whenever the boron atom has some negative partial charge it means certain extent of electron population has been transferred form the adjacent atoms, (that they are sometimes nitrogen, sometimes carbon atoms) to the boron atom. The π-conjugation of parent phenanthrene skeleton is perturbed in various extents by the presence of heteroatoms depending on the location of the centric perturbations have occurred. Thus the charges and bond lengths in the structures are highly dependent on the fine topologies of the systems considered (see Figure 3 and Table 3).

Some bond lengths of the structures considered are listed in Table 3. The shortest B-N bond happens in structer-1 whereas the longest in structures 10 and 11, in which boron atom is mutually shared by two hexagonal rings.

Table 3. Some bond lengths of the structures considered.

No	B-N length	B-C length
1	1.284	1.513
2	1.461	1.510
3	1.483	1.465
4	1.444	1.526, 1.527
5	1.464	1.492
6	1.320	1.427
7	1.321	1.429
8	1.302	1.462
9	1.300	1.456
10	1.492	1.516, 1.516
11	1.492	1.513, 1.516

In Å units.

Note that structures 1,6,7,8 and 9 fall in to the class of $C_{12}H_8BN$ type isomers (boron is on the fusion point except structure-1) whereas structures 2,3,4,5,10,11 are $C_{12}H_{10}BN$ type (boron is on the peripheral circuit) isomers.

Figure 4 shows the calculated IR spectra of the structures considered. In the spectrums aromatic C-H stretchings occur at 3500-3000 cm^{-1}. In structure-2, the peak at 3568 cm^{-1} is N-H stretching. It occurs at 3587 cm^{-1} in structure-4. The B-H stretching happens at 2619 cm^{-1} in 5. The skeletal vibrations of hetero ring of structure-1 is at 1803 cm^{-1} but for the others they are at 1600-1500 cm^{-1} and overlapped with other skeletal breathing vibrations.

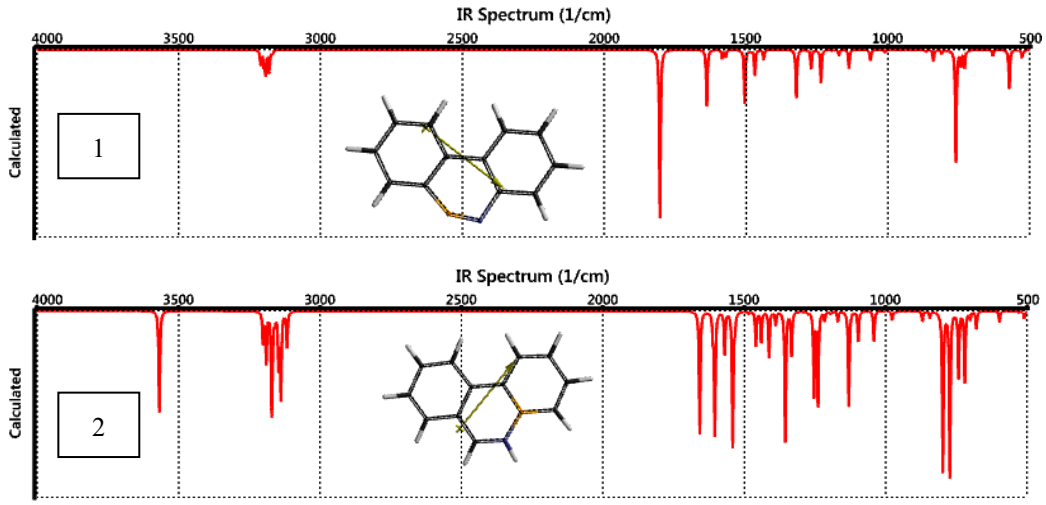

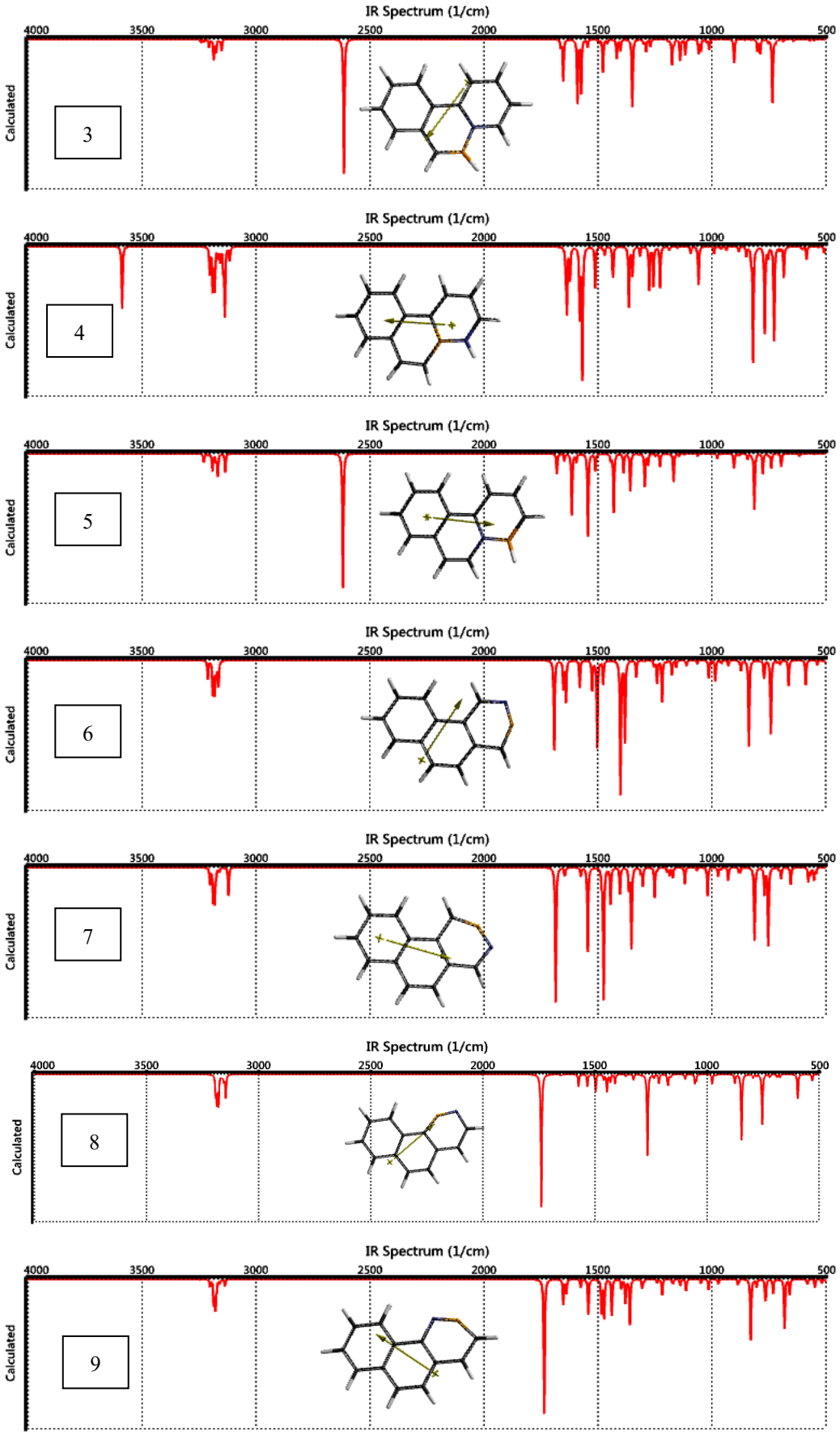
IR Spectrum (1/cm)
4000
3500
3000
2500
2000
1500
1000
500
Calculated
3
IR Spectrum (1/cm)
4000
3500
3000
2500
2000
1500
1000
500
Calculated
4
IR Spectrum (1/cm)
4000
3500
3000
2500
2000
1500
1000
500
Calculated
5
IR Spectrum (1/cm)
4000
3500
3000
2500
2000
1500
1000
500
Calculated
6
IR Spectrum (1/cm)
4000
3500
3000
2500
2000
1500
1000
500
Calculated
7
IR Spectrum (1/cm)
4000
3500
3000
2500
2000
1500
1000
500
Calculated
8
IR Spectrum (1/cm)
4000
3500
3000
2500
2000
1500
1000
500
Calculated
9

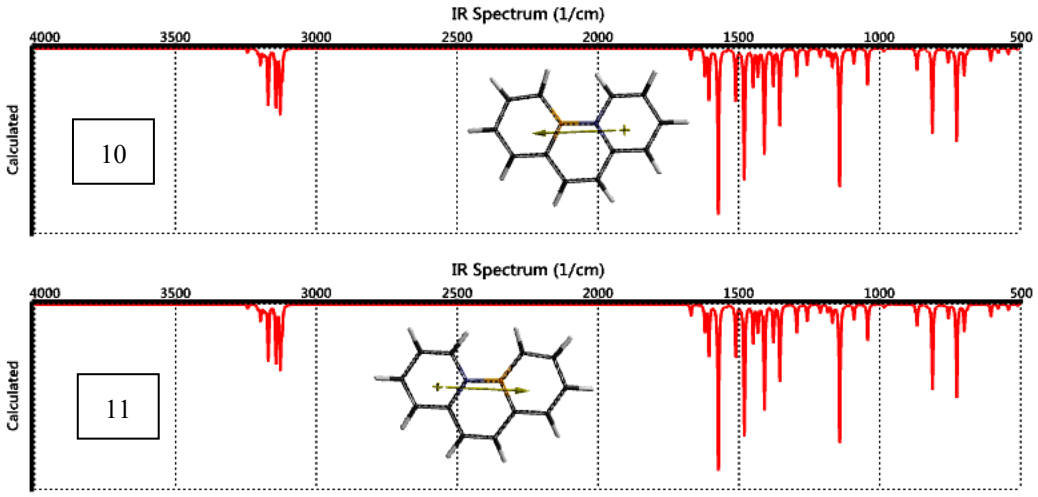

Figure 4. Calculated IR spectra of the structures considered.

Table 4 lists some calculated properties of the structures considered. It is worth mentioning that the polar surface area (PSA) is defined as the amount of molecular surface area arising from polar atoms (N,O) together with their attached hydrogen atoms [31]. Their PSA values differ from each other, meaning that the same kind of atoms might be influenced by electronic factors differently at different positions. The polarizability is defined according to a multivariable formula [21] which is the functions of van der Waals volume and hardness, respectively. The later one is dictated by energies of the highest occupied (HOMO) and the lowest unoccupied (LUMO) molecular orbitals [31].

Table 4. Some properties of the structures considered.

	Dipole moment	Polarizability	Cv (J/mol°)	Area (Å²)	Volume (Å³)	PSA (Å²)	Ovality
1	2.69	56.26	138.71	201.76	196.21	7.054	1.24
2	3.23	56.90	145.33	207.86	201.05	10.676	1.25
3	3.30	57.02	145.07	207.99	202.49	0.517	1.25
4	2.43	56.73	144.94	207.89	201.08	10.718	1.25
5	2.49	56.87	144.66	208.33	202.57	0.518	1.25
6	1.71	56.27	139.02	200.83	195.97	7.145	1.23
7	1.76	56.29	139.26	200.72	195.86	7.294	1.23
8	2.52	56.25	138.28	202.73	196.29	7.200	1.24
9	1.67	56.31	139.40	203.07	196.39	6.449	1.24
10	3.55	56.97	144.67	208.51	202.43	0.525	1.25
11	3.55	56.97	144.67	208.51	202.43	0.525	1.25

Dipole moments in debye units. Polarizabilities in 10^{-30} m^3 units.

Figure 5 shows some of the molecular orbital energy levels of the structures considered. It would be worth remembering that in structures 2,4,10 and 11 the boron atom occupies a fusion point whereas in structures 1,3,5,6,7,8 and 9) a peripheral position.

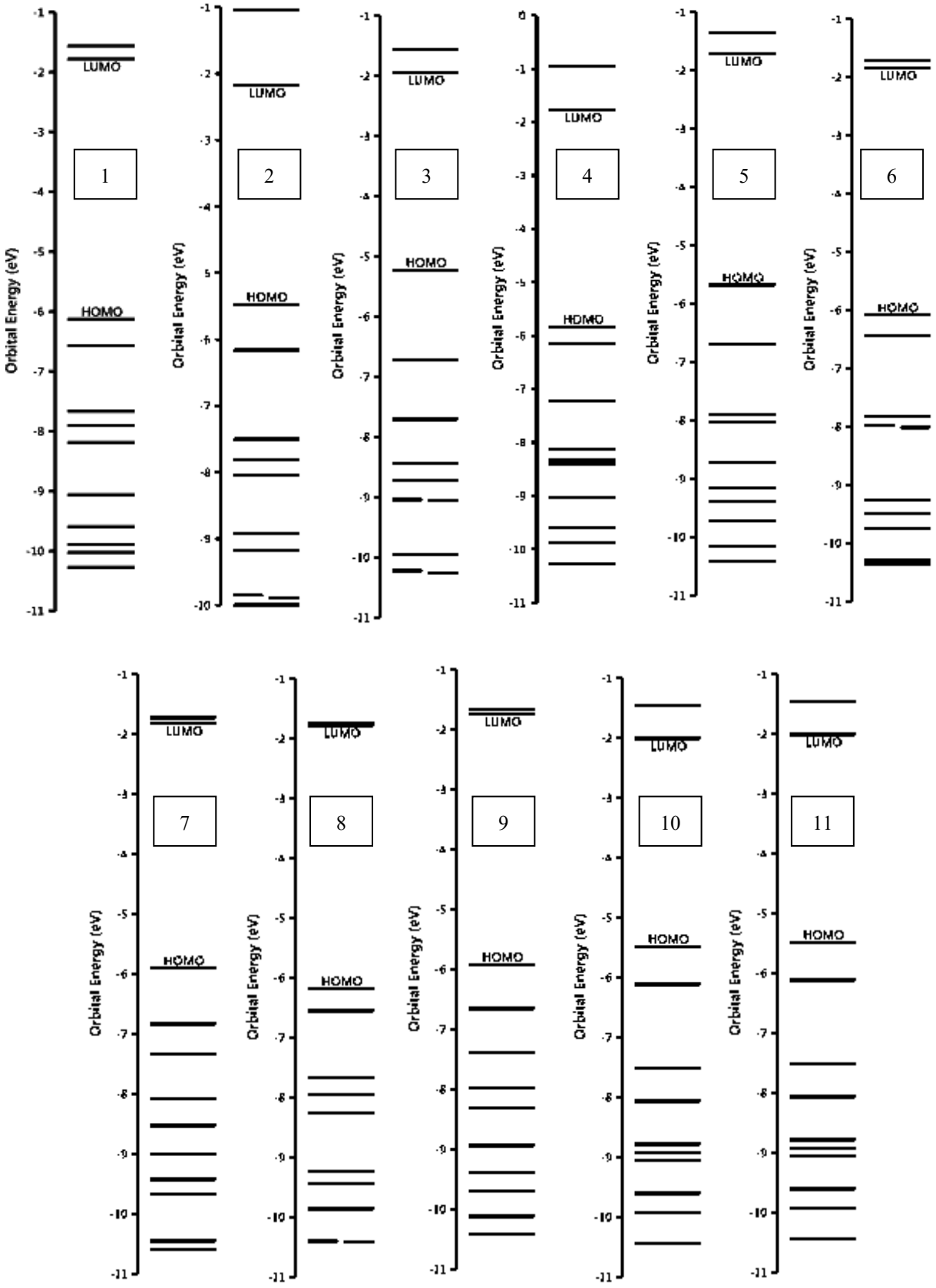

Figure 5. Some of the molecular orbital energy levels of the structures considered.

Table 5 includes the HOMO, LUMO energies and interfrontier molecular orbital energy gap values, Δε (Δε = ε_{LUMO}-ε_{HOMO}) of the structures considered. The algebraic orders of the HOMO and LUMO energies are

8<1<6<9<7<4<10=11<2<3<5 and 2<10=11<3<5<6<7<1<8=4<9, respectively. Consequently the order of Δε values becomes 8>1>6>9>7>4>5>10=11>2>3. Thus, $C_{12}H_8BN$ type isomers (1,6,7,8,9) have greater Δε values than $C_{12}H_8BN$ types (2,3,4,5,10,11). Since the electro negativities of the heteroatoms affect the frontier molecular energy levels, their positions in the π-circuit dictate the HOMO and LUMO energy levels and as a result the energy gap values. The largest Δε having structures 8 and 1 reside in $C_{12}H_8BN$ group of isomers and they possess the boron atom at the peripheral circuit.

Table 5. The HOMO, LUMO energies and Δε values of the structures considered.

No	HOMO	LUMO	Δε
1	-591.24	-171.89	419.35
2	-528.00	-209.48	318.52
3	-503.91	-186.87	317.04
4	-562.61	-171.29	391.32
5	-165.72	179.03	344.75
6	-587.02	-177.07	409.95
7	-569.65	-175.11	394.54
8	-596.61	-171.29	425.32
9	-571.11	-167.36	403.75
10	-528.87	-193.60	335.27
11	-528.87	-193.60	335.27

Energies in kJ/mol.

Figure 6 displays the calculated UV-VIS spectra (time dependent density functional, TDDFT) of the structures considered. They are confined to below 500 nm, having shoulders. Note that the calculated intensities of the peaks are related to magnitudes of the transition moments between the orbitals involved which vary from isomer to isomer [35,36].

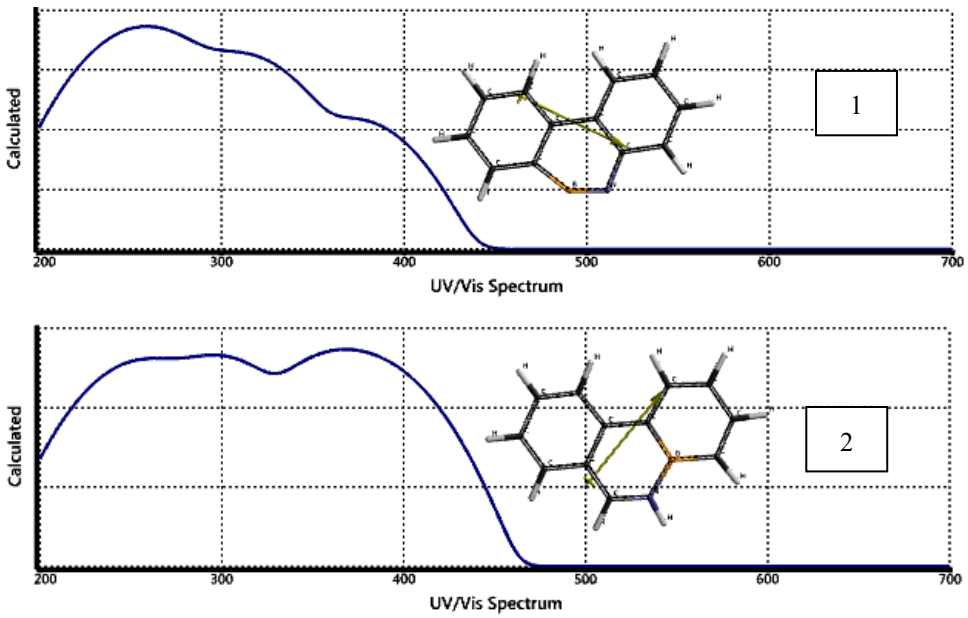

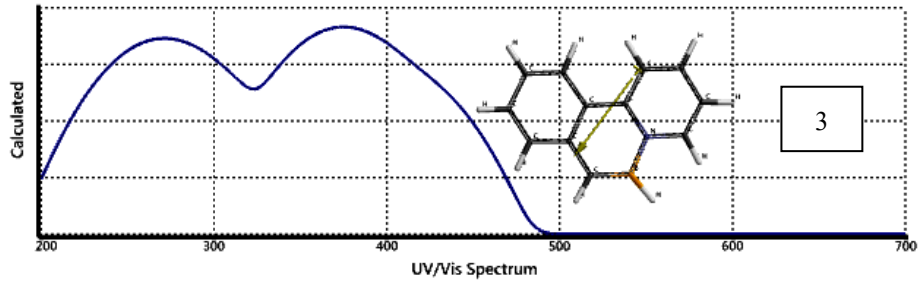
Calculated
200
300
400
500
600
700
UV/Vis Spectrum
3

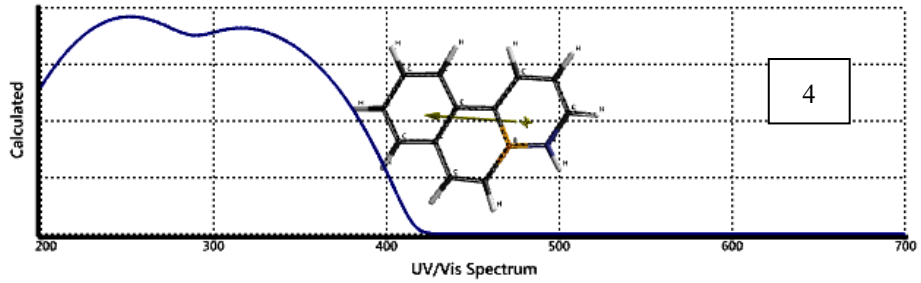
Calculated
200
300
400
500
600
700
UV/Vis Spectrum
4

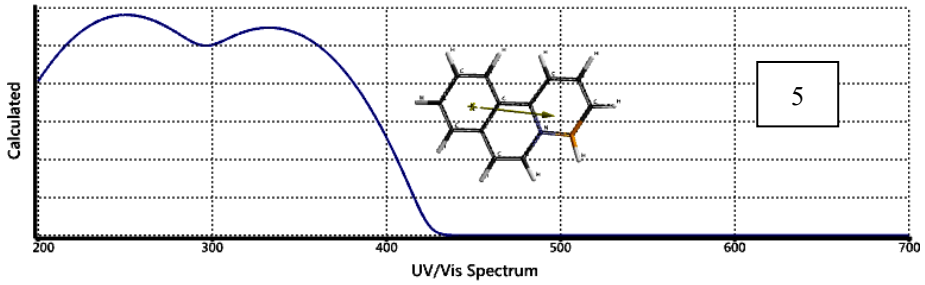
Calculated
200
300
400
500
600
700
UV/Vis Spectrum
5

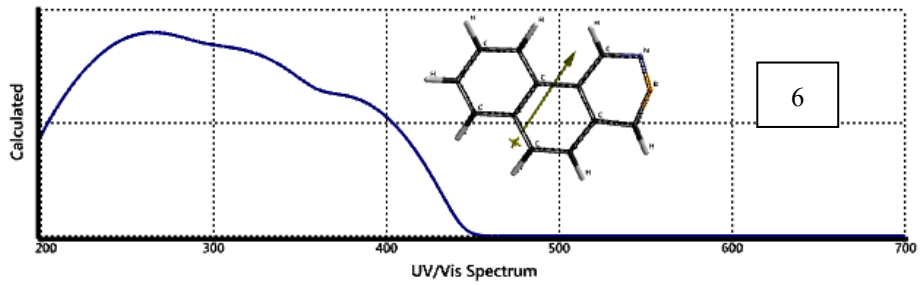
Calculated
200
300
400
500
600
700
UV/Vis Spectrum
6

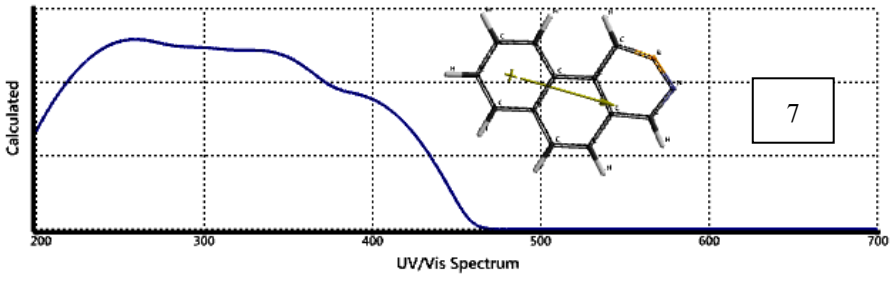
Calculated
200
300
400
500
600
700
UV/Vis Spectrum
7

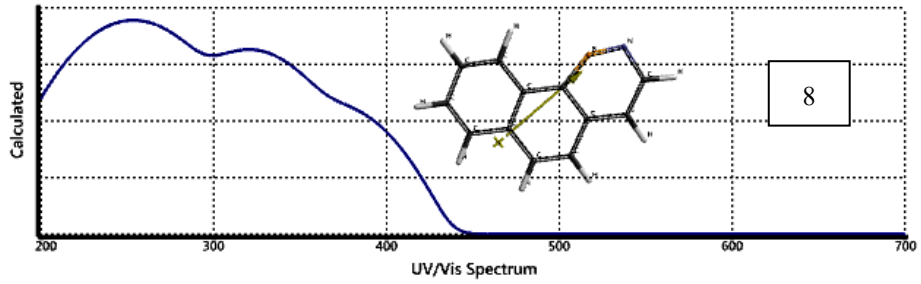
Calculated
200
300
400
500
600
700
UV/Vis Spectrum
8

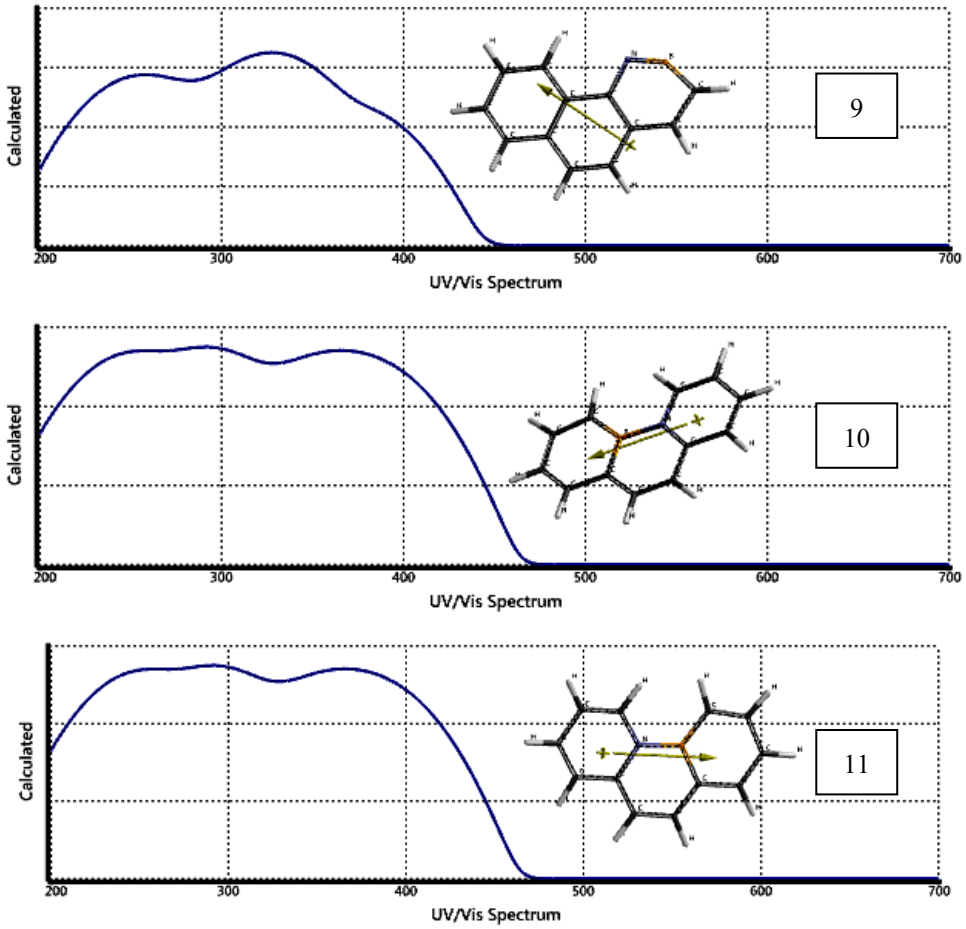

Figure 6. The calculated UV-VIS spectra of the structures considered.

NICS

In 1996, Schleyer has introduced a simple but efficient probe for aromaticity that is "nucleus-independent chemical shift" (NICS) [37]. It is the computed value of the negative magnetic shielding at some selected point in space which is generally, at a ring or cage center. The calculated data piled in the literature through the years indicate that negative NICS values denote aromaticity (-11.5 for benzene, -11.4 for naphthalene) whereas positive NICS values denote antiaromaticity (28.8 for cyclobutadiene) while small NICS values indicate non-aromaticity (-2.1 for cyclohexane, -1.1 for adamantane). NICS may be a useful indicator of aromaticity that usually correlates successfully with the other energetic, structural and magnetic criteria for aromaticity [38-41]. Resonance energies and magnetic susceptibilities measure the overall aromaticity of a polycycle, but do not provide any information about the individual rings. In contrast, NICS has been proved to be an effective probe for local aromaticity of individual rings of polycyclic systems. Several publications exist in the literature that generally aromaticity has been discussed in terms of energetic, structural and magnetic criteria [42-47].

Labeling of the phenanthrene rings is shown in Figure 7 and Table 6 lists NICS (0) values of the rings of the structures considered. It is worth remembering that isomers of $C_{12}H_8BN$ type possess the boron atom at the fusion point of the rings.

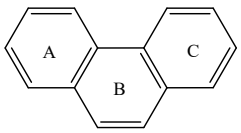

Figure 7. Labeling of the phenanthrene rings.

Table 6 lists the NICS (0) values of the rings and the relative local aromaticity order of the structures considered.

Table 6. NICS (0) values of the rings of the structures considered.

No	Bruto formula	Rings			Local aromaticity order
		A	B	C	
1	$C_{12}H_8BN$	-8.2291	-7.7314	-8.6548	C>A>B
2	$C_{12}H_{10}BN$	-6.4126	-7.9704	-6.7191	B>C>A
3	$C_{12}H_{10}BN$	-6.5767	-7.2549	-4.9623	B>A>C
4	$C_{12}H_{10}BN$	-7.8985	-1.9571	-6.5473	A>C>B
5	$C_{12}H_{10}BN$	-7.6855	-1.0352	-6.1150	A>C>B
6	$C_{12}H_8BN$	-8.3312	-4.7451	-12.4922	C>A>B
7	$C_{12}H_8BN$	-8.4194	-4.8992	-11.9212	C>A>B
8	$C_{12}H_8BN$	-8.6509	-6.2805	-11.4200	C>A>B
9	$C_{12}H_8BN$	-8.7764	6.5528	-10.5935	C>A>B
10	$C_{12}H_{10}BN$	-6.2575	-7.5312	-4.1689	B>A>C
11	$C_{12}H_{10}BN$	-4.1689	-7.5312	-6.2575	B>C>A

With the exception of isomer-1, the rings of $C_{12}H_8BN$ isomers (1,6,7,8 and 9) having the BN bond is characterized with the highest local aromaticity.

Figure 8 displays the bond densities of the structures considered. The figure indicates the existence of appreciable bond density between the nitrogen and the boron atoms although greater density localizes on the nitrogen atom. In some cases hyperconjugative effects are operative. There are number of indications that empty boron *p*-orbital, such as in trialkyl boron compounds, invite hypercojugation with neighboring C-H bonds [48]. On the other hand, stabilities of aromatic structures are also highly affected by the number of Clar's sextets [49,50]. Thus, not only the position of the BN-bond but also their relative position in the π-conjugation in the structure implicitly affect the fine topology hence govern various properties of the structure of consideration.

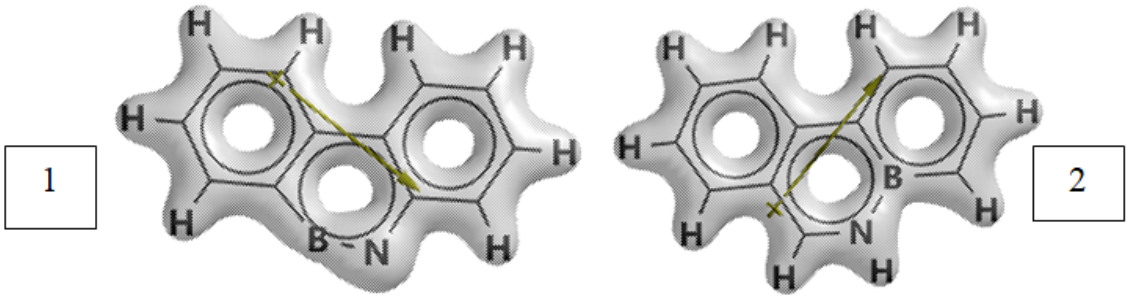

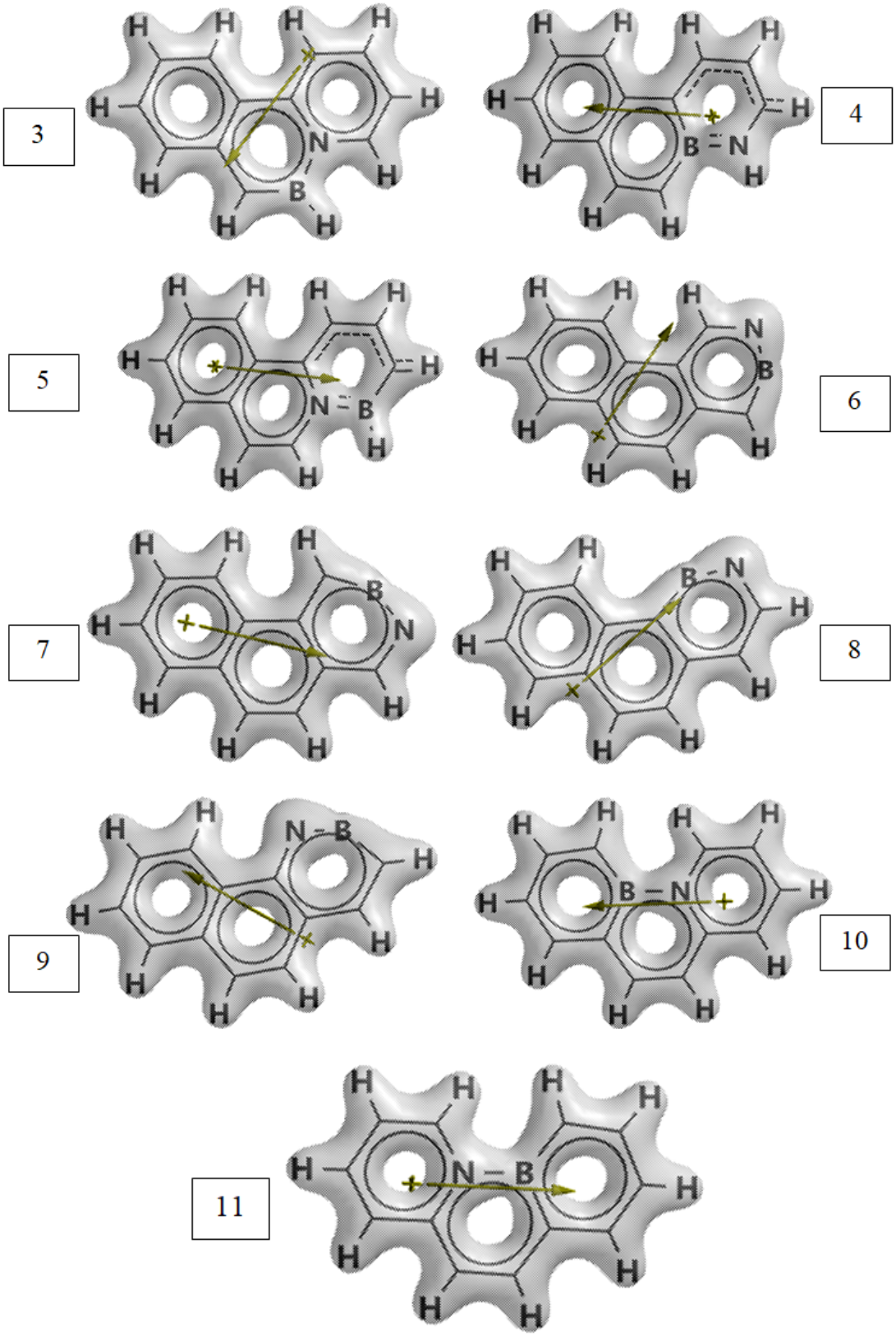

Figure 8. The bond densities of the structures considered.

4. Conclusion

The present computational study considered various isomeric B-N bond embedded phenanthrene systems within the restrictions of density functional theory at the level of B3LYP/6-311++G(d,p). All of the isomers possess exothermic H^o and favorable G^o values and as well as they are electronically stable. The calculated B-N and B-C bond lengths vary in 1.28-1.49 Å and 1.45-1.51 Å, respectively. As most of the properties, their HOMO and LUMO energies are dictated by the fine topology of the structures considered. However, the largest inter frontier molecular orbital energy gap, $\Delta\varepsilon$, values possessed by structures in which the boron atom involved in the peripheral circuit of $C_{12}H_8BN$ type isomers. The calculated UV-VIS spectra of all the structures confined to region of 200-500 nm, which show some shoulders. Generally, $C_{12}H_8BN$ type isomers having the embedded BN bond is characterized with rings having the highest local aromaticity compared to the ones of $C_{12}H_{10}BN$ type.

In general various properties of those structures are dictated by their fine topologies governed by structural and electronic factors arising from the B-N linkage.

References

[1] Gsänger, M., Bialas, D., Huang, L., Stolte, M., & Würthner, F. (2016). Organic semiconductors based on dyes and color pigments. *Adv. Mater., 28*, 3615–3645. https://doi.org/10.1002/adma.201505440

[2] Li, M., An, C., Pisula, W., & Müllen, K. (2018). Cyclopentadithiophene-benzothiadiazole donor-acceptor polymers as prototypical semiconductors for high-performance field-effect transistors. *Acc. Chem. Res*., *51*, 1196–1205. https://doi.org/10.1021/acs.accounts.8b00025

[3] Grimsdale, A.C., Chan, K.L., Martin, R.Ei, Jokisz, P.G., Holmes, A.B. (2009). Synthesis of light-emitting conjugated polymers for applications in electroluminescent devices. *Chem. Rev.*, *109*(3), 897–1091. https://doi.org/10.1021/cr000013v

[4] Lu, L., Zheng, T., Wu, Q., Schneider, A.M., Zhao, D., & Yu, L. (2015). Recent advances in bulk heterojunction polymer solar cells. *Chem. Rev., 115*, 12666–12731. https://doi.org/10.1021/acs.chemrev.5b00098

[5] Zhan, C., & Yao, J. (2016). More than conformational "Twisting" or "Coplanarity": molecular strategies for designing high-efficiency nonfullerene organic solar cells. *Chem. Mater.*, *28*, 1948–1964. https://doi.org/10.1021/acs.chemmater.5b04339

[6] Shi, K., Zhang, F., Di, C.A., Yan, T.W., Zou, Y., Zhou, X., Zhu, D., Wang, J.Y., & Pei, J. (2015). Toward high performance n-type thermoelectric materials by rational modification of BDPPV backbones. *J. Am. Chem. Soc., 137*(22), 6979–82. https://doi.org/10.1021/jacs.5b00945

[7] Huang, D., Wang, C., Zou, Y., Shen, X., Zang, Y., Shen, H., Gao, X., Yi, Y., Xu, W., Di, C.A., & Zhu D. (2016). Bismuth interfacial doping of organic small molecules for high performance n-type thermoelectric materials. *Angew. Chem. Int. Ed. Engl*., *55*(36), 10672–5. https://doi.org/10.1002/anie.201604478

[8] Lim, E., Peterson, K.A., Su, G.M., & Chabinyc, M.L. (2018). Thermoelectric properties of poly(3-hexylthiophene) (P3HT) doped with 2,3,5,6-tetrafluoro-7,7,8,8-tetracyanoquinodimethane (F4TCNQ) by vapor-phase infiltration. *Chem. Mater., 30*, 998–1010. https://doi.org/10.1021/acs.chemmater.7b04849

[9] Wang, X., Lv, L., Li, L., Chen, Y., Zhang, K., Chen, H., Dong, H., Huang, J., Shen, G., Yang, Z., Huang, H. (2016). High-performance all-polymer photo response devices based on acceptor-acceptor conjugated polymers. *Adv. Funct. Mater., 26*, 6306–6315. https://doi.org/10.1002/adfm.201601745

[10] Benavides, C.M., Murto, P., Chochos, C.L., Gregoriou, V.G., Avgeropoulos, A., Xu, X., Bini, K., Sharma, A., Andersson, M.R., Schmidt, O., Brabec, C.J., Wang, E., & Tedde, S.F. (2018). High-performance organic photo detectors from a high-band gap indacenodithiophene-based π-conjugated donor-acceptor polymer. *ACS Appl. Mater. Interfaces, 10*, 12937–12946. https://doi.org/10.1021/acsami.8b03824

[11] Murto, P., Genene, Z., Benavides, C.M., Xu, X., Sharma, A., Pan, X., Schmidt, O., Brabec, C.J., Andersson, M.R., Tedde, S.F., Mammo, W., & Wang, E. (2018). High performance all-polymer photo detector comprising a donor-acceptor-acceptor structured indacenodithiophene-bithieno[3,4-c]pyrroletetrone copolymer. *ACS Macro Lett., 7*, 395–400. https://doi.org/10.1021/acsmacrolett.8b00009

[12] Zachary, X.G., & Shih-Yuan, L. (2018). The state of the art in azaborine chemistry: New synthetic methods and applications. *Journal of the American Chemical Society*, *140* (4), 1184–1194. https://doi.org/10.1021/jacs.7b09446

[13] Huang, J., & Li, Y. (2018). BN embedded polycyclic π-conjugated systems: Synthesis, optoelectronic properties, and photovoltaic applications. *Frontiers in Chemistry*, *6*, 341. https://doi.org/10.3389/fchem.2018.00341

[14] Edel, K., Yang, X., Ishibashi, J.S.A., Lamm, A.N., Maichle-Mössmer, C., Giustra, Z.X., Liu, S.Y., & Bettinger, H.F. (2018). The Dewar isomer of 1,2-dihydro-1,2- azaborinines: isolation, fragmentation, and energy storage. *Angew. Chem. Int. Ed. Engl.*, *57*(19), 5296–5300. https://doi.org/10.1002/anie.201712683

[15] Burford, R.J., Li, B., Vasiliu, M., Dixon, D.A., & Liu, S.Y. (2015). Diels-Alder reactions of 1,2-azaborines. *Angew. Chem. Int. Ed. Engl.*, *54*(27), 7823–7. https://doi.org/10.1002/anie.201503483

[16] Chen, C., Du, C-Z., & Wang, X-Y. (2022). The Rise of 1,4-BN-Heteroarenes: Synthesis, Properties, and Applications. *Adv. Sci.*, *9*, 2200707 (1–22). https://doi.org/10.1002/advs.202200707

[17] Wang, X.Y., Wang, J.Y., & Pei, J. (2015). BN heterosuperbenzenes: synthesis and properties. *Chemistry–A European Journal*, *21*(9), 3528–3539.

[18] Helten, H. (2016). B=N Units as part of extended π-conjugated oligomers and polymers. *Chemistry–A European Journal*, *22*(37), 12972–12982.

[19] Bélanger-Chabot, G., Braunschweig, H., & Roy, D.K. (2017). Recent developments in azaborinine chemistry. *European Journal of Inorganic Chemistry*, *2017*(38-39), 4353–4368.

[20] McConnell, C.R., & Liu, S.Y. (2019). Late-stage functionalization of BN-heterocycles. *Chemical Society Reviews*, *48*(13), 3436–3453.

[21] Abengózar, A., García-García, P., Fernández-Rodríguez, M.A, Sucunza, D., & Vaquero, J.J. (2021). In *Advances in Heterocyclic Chemistry*, Vol. 135 (Eds: E. F. V. Scriven, C.A. Ramsden), San Diego; Academic Press, p. 197.

[22] Bhattacharjee, A., Davies, G.H., Saeednia, B., Wisniewski, S.R., & Molander, G.A. (2021). Selectivity in the elaboration of bicyclic borazarenes. *Advanced Synthesis & Catalysis*, *363*(9), 2256–2273.

[23] Stewart, J.J.P. (1989). Optimization of parameters for semi-empirical methods I. *J. Comput. Chem.*, *10*, 209–220. https://doi.org/10.1002/jcc.540100208

[24] Stewart, J.J.P. (1989). Optimization of parameters for semi-empirical methods II. *J. Comput.Chem., 10*, 221–264. https://doi.org/10.1002/jcc.540100209

[25] Leach, A.R. (1997). *Molecular modeling*. Essex: Longman.

[26] Kohn, W., & Sham, L.J. (1965). Self-consistent equations including exchange and correlation effects. *Phys. Rev.*, *140*, 1133–1138. https://doi.org/10.1103/PhysRev.140.A1133

[27] Parr, R.G., & Yang, W. (1989). *Density functional theory of atoms and molecules*. London: Oxford University Press.

[28] Becke, A.D. (1988). Density-functional exchange-energy approximation with correct asymptotic behavior. *Phys. Rev. A*, *38*, 3098–3100. https://doi.org/10.1103/PhysRevA.38.3098

[29] Vosko, S.H., Wilk, L., & Nusair, M. (1980). Accurate spin-dependent electron liquid correlation energies for local spin density calculations: a critical analysis. *Can. J. Phys*., *58*, 1200–1211. https://doi.org/10.1139/p80-159

[30] Lee, C., Yang, W., & Parr, R.G. (1988). Development of the Colle-Salvetti correlation energy formula into a functional of the electron density. *Phys. Rev. B*, *37*, 785–789. https://doi.org/10.1103/PhysRevB.37.785

[31] SPARTAN 06 (2006). Wavefunction Inc. Irvine CA, USA.

[32] Gaussian 03, Frisch, M.J., Trucks, G.W., Schlegel, H.B., Scuseria, G.E., Robb, M.A.,Cheeseman, J.R.,Montgomery, Jr., J.A., Vreven, T., Kudin, K.N., Burant, J.C., Millam, J.M., Iyengar, S.S., Tomasi, J., Barone, V.,Mennucci, B., Cossi, M., Scalmani, G., Rega, N., Petersson, G.A., Nakatsuji, H., Hada, M., Ehara, M., Toyota, K.,Fukuda, R., Hasegawa, J., Ishida, M., Nakajima, T., Honda, Y., Kitao, O., Nakai, H., Klene, M., Li, X., Knox,J.E., Hratchian, H.P., Cross, J.B., Bakken, V., Adamo, C., Jaramillo, J., Gomperts, R., Stratmann, R.E., Yazyev, O., Austin, A.J., Cammi, R., Pomelli, C., Ochterski, J.W., Ayala, P.Y., Morokuma, K., Voth, G.A., Salvador, P.,Dannenberg, J.J., Zakrzewski, V.G., Dapprich, S., Daniels, A.D., Strain, M.C., Farkas, O., Malick, D.K., Rabuck, A.D., Raghavachari, K., Foresman, J.B., Ortiz, J.V., Cui, Q., Baboul, A.G., Clifford, S., Cioslowski, J., Stefanov, B.B., Liu, G., Liashenko, A., Piskorz, P., Komaromi, I., Martin, R.L., Fox, D.J., Keith, T., Al-Laham, M.A., Peng, C.Y., Nanayakkara, A., Challacombe, M., Gill, P.M.W., Johnson, B., Chen, W., Wong, M.W., Gonzalez, C., &Pople, J.A., Gaussian, Inc., Wallingford CT, 2004.

[33] Dewar, M.J.S. (1969). *The molecular orbital theory of organic chemistry*. New York: McGraw-Hill,

[34] Dewar, M.J.S., & Dougherty, R.C. (1975). *The PMO theory of organic chemistry*. New York: Plenum-Rosetta. https://doi.org/10.1007/978-1-4613-4404-9

[35] Anslyn, E.V., & Dougherty, D.A. (2006). *Modern physical organic chemistry*. Sausalito, California: University Science Books.

[36] Turro, N.J. (1991). *Modern molecular photochemistry.* Sausalito: University Science Books.

[37] Schleyer, P.R., Maerker, C., Dransfeld, A., Jiao, H., & Hommes, N.J.R.E. (1996). Nucleusindependent chemical shifts: A simple and efficient aromaticity probe, *J. Am. Chem. Soc*. *118,* 6317–6318. https://doi.org/10.1021/ja960582d

[38] Jiao, H., & Schleyer, P.R. (1998). Aromaticity of pericyclic reaction transition structures: magnetic evidence, *J. Phys. Org. Chem*. 11, 655–662. https://doi.org/10.1002/(SICI)1099-1395(199808/09)11:8/9<655::AIDPOC66>3.0.CO;2U

[39] Schleyer, P.R., Kiran, B., Simion, D.V., and Sorensen, T.S. (2000). Does Cr(CO)3 complexation reduce the aromaticity of benzene?, *J. Am. Chem. Soc*. 122, 510–513. https://doi.org/10.1021/ja9921423

[40] Quinonero, D., Garau, C., Frontera, A., Ballaster, P., Costa, A., & and Deya, P.M. (2002). Quantification of aromaticity in oxocarbons: The problem of the fictitious “nonaromatic” reference system, *Chem. Eur. J. 8*, 433–438. https://doi.org/10.1002/1521-3765(20020118)8:2<433::AID-CHEM433>3.0.CO;2-T

[41] Patchkovskii, S., & Thiel, W. (2002). Nucleus-independent chemical shifts from semiempirical calculations, *J. Mol. Model. 6*, 67–75. https://doi.org/10.1007/PL00010736

[42] Minkin, V.I., Glukhovtsev, M.N., & Simkin, B.Y. (1994). *Aromaticity and antiaromaticity: Electronic and structural aspects*. New York: Wiley.

[43] Schleyer, P.R., & Jiao, H. (1996). What is aromaticity?, *Pure Appl. Chem*. *68*, 209–218. https://doi.org/10.1351/pac199668020209

[44] Glukhovtsev, M.N. (1997). Aromaticity today: energetic and structural criteria, *J. Chem Educ*. *74*, 132–136. https://doi.org/10.1021/ed074p132

[45] Krygowski, T.M., Cyranski, M.K., Czarnocki, Z., Hafelinger, G., & Katritzky, A.R. (2000). Aromaticity: a theoretical concept of immense practical importance, *Tetrahedron 56*, 1783–1796. https://doi.org/10.1016/S0040-4020(99)00979-5

[45] Schleyer, P.R. (2001). Introduction: Aromaticity, *Chem. Rev*. *101*, 1115–1118. https://doi.org/10.1021/cr0103221

[47] Cyranski, M.K., Krygowski, T.M., Katritzky, A.R., & Schleyer, P.R. (2002). To what extent can aromaticity be defined uniquely?, *J. Org. Chem*. *67*, 1333–1338. https://doi.org/10.1021/jo016255s

[48] Onak, T. (1975). *Organoborane chemistry*. New York: Academic Press.

[49] Clar, E. (1972). The aromatic sextet. London: Wiley.

[50] Clar, E. (1964). Polycyclic hydrocarbons, V1. London: Academic Press.